analytical chemistry

ARTICLE

pubs.acs.org/ac

# Gold Nanoparticle Enhanced Electrochemiluminescence of CdS Thin Films for Ultrasensitive Thrombin Detection

Jing Wang, Yun Shan, Wei-Wei Zhao, Jing-Juan Xu,* and Hong-Yuan Chen

Key Laboratory of Analytical Chemistry for Life Science, School of Chemistry and Chemical Engineering, Nanjing University, Nanjing 210093, China

**ABSTRACT:** Interactions between surface plasmons (SP) of metallic surfaces and photoluminescence (PL) of semiconductor nanocrystal (S-NC) surfaces have been extensively investigated, and SP-induced PL enhancement has been used as a sensitive analytical technique. However, this SP induced electrochemiluminescence (ECL) enhancement is rarely studied. In this work, we report greatly enhanced ECL of CdS thin films by gold nanoparticles (Au NPs) for ultrasensitive detection of thrombin. The system was composed of a CdS NC film on glassy carbon electrode (GCE) as ECL emitter attached an aptamer of thrombin. Then, ssDNA−AuNP conjugates hybridized with the aptamer to form a separation length of ca. 12 nm between CdS NCs and Au NPs. The system showed 5-fold enhancement of ECL intensity as compared to that without Au NPs, which might be attributed to the long-distance interaction between the S-NCs and SPR field of noble metal nanoparticles (MNPs).We also found that the enhanced ECL could be influenced by the involving factors such as the separation distance, spectral overlap, and magnetic field. Such enhancement in combination with smart recognition of aptamer and target protein allowed us to construct an ultrasensitive aptasensor for attomolar detection of thrombin. The presence of target protein was reflected by the ECL signal decrease caused by the target-induced removal of ssDNA−AuNP conjugates. The decrease of ECL signal was logarithmically linear with the concentration of thrombin in a wide range from 100 aM to 100 fM. The principle described in this work could be also applied to many other bioassays.

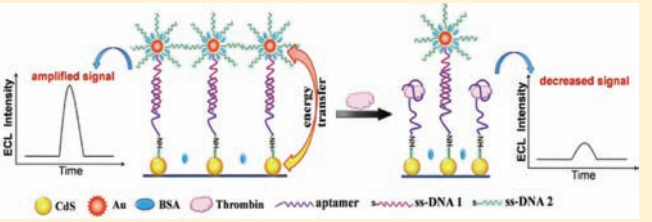


In recent years, considerable attention from the fundamental physical perspective has been given to the semiconductor nanocrystals (S-NCs)/metal systems.[1−6] One interesting topic relating to the system is the exploitation of optical behavior of S-NCs near or in contact with nanostructural metallic (Au, Ag) surfaces.[7−9] As the energy transfer between the excitons in the S-NCs and plasmons in the metal surface occurs, the optical properties of S-NCs near the metal surface could be modified significantly by controlling the nanoscale-localized energy transfer at the interface. Previous studies have shown that interactions with surface plasmons (SP) of metallic (Au, Ag) surfaces can greatly affect the photoluminescence (PL) intensities of S-NCs, in which PL intensity of the S-NCs is either enhanced or diminished by the proximal metal nanoparticles (MNPs) due to the competition between field enhancement and Förster resonance energy transfer (FRET).[5,7,10] When the S-NCs and MNPs are at close proximity, PL emission of S-NCs can be easily quenched through nonradiative energy dissipation in the metal. However, when they are separated at a certain distance, excitation of a MNP surface plasmon resonance (SPR) can create strong local electric fields that in turn modulate the PL response of the S-NCs by the manner in which the photoexcitation can be converted into fluorescence. Consequently, the PL signals are greatly amplified. This SP-induced PL enhancement has been extensively used as a sensitive analytical technique in molecular science, biology, and medicine.[11,12]

Electrogenerated chemiluminescence (electrochemiluminescence or ECL) of S-NCs would also be influenced by nearby MNPs. ECL is a light emission that arises from the high-energy electron transfer reaction between electrogenerated species, having advantages of excellent temporal and spatial controllability.[13,14] Compared with PL methods, ECL does not need a light source; it, thus, is not involved with the problems of scattered light and luminescent impurities. These superiorities make ECL a desirable analytical tool for sensitive biomolecules detection, which is the pursuit of analytical chemistry for life science.[15−18] Lately, our group has first demonstrated the existence of the interactions between electrogenerated excitons in ECL of CdS/Mn NCs and ECL-induced SPR of Au NPs. In that work, ECL intensity from CdS/Mn NC film was increased by 55% (about 1.5-fold enhancement) when Au NPs and CdS/Mn NC film were at a distance about the length of 10 nm.[19] However, this enhancement efficiency of ECL emission was much less than that of PL. Since the PL emission is dominated by excitation and emission within the S-NC core while ECL of S-NCs mainly occurs via surface electron−hole recombination, ECL is much more sensitive to their surface electronic structure than the PL. Therefore, ECL properties of S-NCs are highly dependent on their surface states, which can be

**Received:** November 22, 2010
**Accepted:** April 25, 2011
**Published:** April 25, 2011

**Scheme 1. ECL Aptamer Sensing Platform Based on Energy Transfer between CdS NCs and Au NPs**

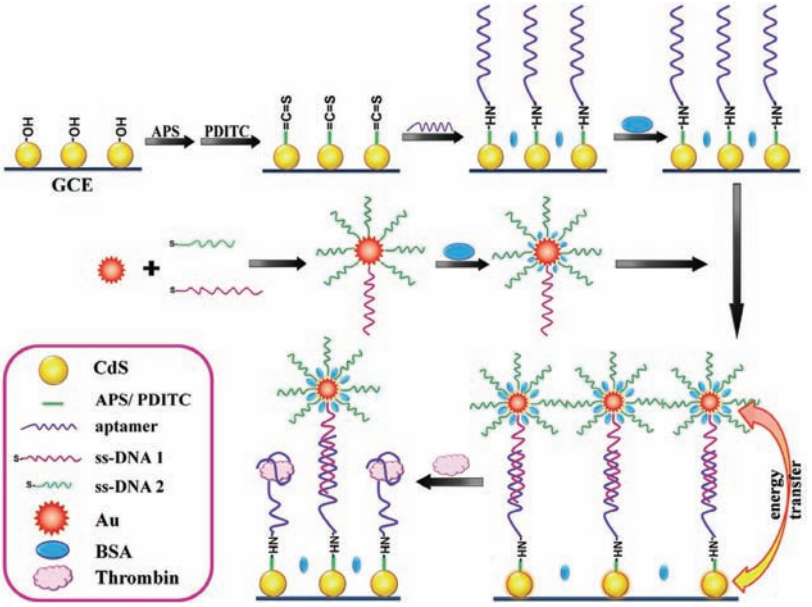


passivated by capping with an organic agent or doping with other materials.[20,21] The passivated surfaces not only have a strong effect on the luminescence peak and efficiency but also have an effect on the electromagnetic field of S-NC surface, which can further influence the SPR when the MNPs are approaching.

Aiming at better understanding of the interaction between ECL of S-NCs and ECL-induced SPR of Au NPs, we further studied the influencing factors of this enhancement, involving separation distance, spectral overlap, and magnetic field. In present work, the CdS NC film as ECL emitter was modified on glassy carbon electrode (GCE) attached to an aptamer of thrombin. Then, its complementary ssDNA in ssDNA−AuNP conjugates hybridized with the aptamer to form a certain distance between CdS NCs and Au NPs (Scheme 1). We showed that ECL emission from CdS NC film could induce SPR of Au NPs, and the induced SPR in turn had 5-fold enhancement of the ECL response of CdS NCs. Meanwhile, we used aptamer as binder to control the distance between CdS NC film and Au NPs due to its unique merits such as simple synthesis and good stability.[22,23] When it was taken advantage of that antithrombin aptamer can specifically bind with thrombin and their interaction was stronger than that between aptamer and its cDNA chain,[24] ultrasensitive detection of thrombin was achieved. The presence of thrombin was sensed by the remarkable decrease of ECL signal which was originated from the replacement of ssDNA−AuNP conjugates by thrombin. The difference of ECL intensity ($\Delta I$) before and after the replacement was correlated to the concentration of thrombin. This ECL aptasensor based on CdS NC film displays high specificity and wide linear range. Some works had reported the ECL thrombin detection using the thrombin as the binding agent of ECL emitter.[23,25−27] Yet, in these reports, the ruthenium complex was usually employed whereas S-NCs were seldom exploited as ECL emitter to date.[26] Herein, the ECL signal of S-NCs could be effectively amplified based on the SPR-field enhancement by Au NPs, and thrombin with extremely low concentration could be ultrasensitively detected. This work would add new insights into the understanding of exciton−SPR interactions and open up the possibility for the design of more efficient ECL biosensors.

## EXPERIMENTAL SECTION

**Reagents.** Labeled DNA oligonucleotides were purchased from Shenggong Bioengineering Ltd. Company (Shanghai, China). Two different aptamers, which could recognize different positions of thrombin, were reported.[28] The sequences of these oligonucleotides employed are given below. (Aptamer 1 and aptamer 2 were partially complementary with ssDNA 1 and ssDNA 2, respectively. ssDNA 3 was complementary with ssDNA 3′. Italic nucleotides were complementary.)

- 30-Mer amino modified anti-thrombin aptamer (aptamer 1):

  5'-$NH_2$-$(CH_2)_6$-GTAGCCGTGGTA*GGGCAGGTTGGGGTGACT* -3'

- 17-Mer amino modified anti-thrombin aptamer (aptamer 2):

  5'-$NH_2$-$(CH_2)_6$-GTGGT*TGGTGTGGTTGG* -3'

- 24-Mer thiol modified partial complementary ssDNA (ssDNA 1):

  5'-SH-$(CH_2)_6$-GTGTGT*AGTCACCCCAACCTGCCC* -3'

- 22-Mer thiol modified partial complementary ssDNA (ssDNA 2):

  5'-SH-$(CH_2)_6$-GTTGGTGAGT*CCAACCACACCA* -3'

- 18-Mer amino modified ssDNA (ssDNA 3)

  5'-$NH_2$-$(CH_2)_6$-*CGTTCCGGTTGCCTACTG* -3'

- 18-Mer thiol modified complementary ssDNA (ssDNA 3')

  5'-SH-$(CH_2)_6$-*CAGTAGGCAACCGGAACG* -3'

- 5'-thiol modified noncomplementary ssDNA (ssDNA B):

  5'-SH-$(CH_2)_6$-GCGCGAACCGTATA -3'


dx.doi.org/10.1021/ac200616g |*Anal. Chem.* 2011, 83, 4004–4011

Thrombin, bovine serum albumin (BSA), hemoglobin (Hb), lysozyme (Lyso), 3-aminopropyl-triethoxysilane (APS), 1,4-di-isothiocyanatobenzene (98%; PDITC), tri(2-carboxyethyl) phosphine hydrochloride (TCEP), and 3-mercapto-1-hexanol (MCH) were purchased from Sigma-Aldrich (St. Louis, MO) and used without further purification. Tris−HCl buffer (0.1 M) containing 0.1 M NaCl and 5 mM $MgCl_2$ (pH 7.4; after abbreviated as $Tris^+$ buffer) was employed for hybridization and preparation of DNA stock solutions. All other reagents were of analytical grade and used as received. Millipore ultrapure water (resistivity ≥18.2 MΩcm) was used throughout the experiment.

**Apparatus.** The electrochemical measurements were recorded with CHI 660A electrochemical workstation (Shanghai CHI Instruments Co., China). The ECL emission measurements were conducted on a model MPI-A electrochemiluminescence analyzer (Xi'An Remax Electronic Science and Technology Co. Ltd., Xi'An, China) at room temperature, and the voltage of the PMT was set at −500 V in the process of detection. All experiments were carried out with a conventional three-electrode system. The working electrode was a 3 mm diameter GCE; Pt wire and SCE electrode served as the counter and reference electrodes, respectively.

Transmission electron microscopy was performed with a JEOL model 2000 instrument operating at 200 kV accelerating voltage. The UV−vis absorption spectra were obtained on a Shimadzu UV-3600 UV-vis−NIR photospectrometer (Shimadzu Co.). PL spectra were obtained on a RF-540 spectrophotometer (Shimadzu Co).

**Preparation of CdS NCs.** Five nanometer CdS NCs were synthesized as in the literature with some modification.[19] Briefly, $Cd(NO_3)_2 \cdot 4H_2O$ (0.1683 g) was dissolved in 30 mL of ultrapure water and heated to 70 °C under stirring; then, the mixture was injected into a freshly prepared solution of $Na_2S$ (0.5960 g) in 30 mL of ultrapure water. Instantly, orange-yellow solution was obtained. The solution was held at 70 °C for 3 h with continuous refluxing. The final reaction precipitates were centrifugated and washed thoroughly with absolute ethanol two times and ultrapure water two times. Then, the obtained precipitate was redispersed into water for centrifugation to collect the upper yellow solution of CdS NCs. The average size of synthesized CdS NCs was about 5 nm, as indicated by UV−vis spectrum and transmission electron microscopy (TEM). Five nanometer 1.34 atom % manganese doped CdS NCs were also synthesized by the way we have reported previously[19] and also characterized by TEM. The final solution was rather stable for 2 months when stored in a refrigerator at 4 °C.

**Synthesis of Au NPs.** Au NPs with average diameter 5 ± 1 nm were prepared through the reduction of $HAuCl_4$ by sodium borohydride ($NaBH_4$) according to the reported methods with slight modifications.[19,29] All glassware used in the synthesis procedures were immersed in freshly prepared aqua regia ($HNO_3$/HCl = 1:3) for 12 h, then washed with ultrapure water, and dried before use. Ice cold 0.1 M $NaBH_4$ (0.6 mL) was added to 20 mL of aqueous solution containing $2.5 \times 10^{-4}$ M $HAuCl_4$ under stirring. The solution immediately turned to an orange-red color, indicating the formation of Au NPs, and was kept stirring in an ice bath for 10 min. Then, the solution reacted at room temperature for another 3 h with the color changing from orange-red to wine red. The nearly monodispersed Au NPs were characterized by TEM. The prepared Au NPs were stored at 4 °C for further use.

**Preparation of ssDNA−AuNP Conjugates.** The ssDNA 1 and ssDNA B (bio bar code) modified with a thiol at their 5′-end were used to prepare ssDNA−AuNP conjugates, with the molar ratio of 1/27/100 for Au NPs/ssDNA 1/ssDNA B.[30] Since ssDNA 1 was complementary to aptamer 1 and ssDNA B was noncomplementary, the low density of ssDNA 1 on AuNP would be favorable to the one-to-one combination of aptamer 1. Briefly, ssDNA 1 (49 μL, 1 μM) and ssDNA B (181 μL, 10 μM) was activated with 1.5 μL of 10 mM TCEP before use, in order to reduce disulfide bonds. Prepared Au NPs (0.3 mL) were added to $Tris^+$ buffer containing ssDNA 1 and ssDNA B. After shaking gently for 16 h, oligonucleotides were covalently attached to Au NPs through Au−S bonding, followed by blocking the Au NPs with 2 wt % bovine serum albumin (BSA) solution. After BSA blocking, the ssDNA−AuNP conjugates were kept in 0.1 M Tris−HCl buffer containing 0.5 M NaCl and 5 mM $MgCl_2$ (pH 7.4) at 4 °C before use.

**Preparation of CdS NCs Film.** The GCE was pretreated before modification by polishing its surface with successively finer grade sand papers and then polished to a mirror smoothness with aqueous slurries of alumina powders (average particle diameters: 0.3 and 0.05 μm $Al_2O_3$) on a polishing silk. The GCE was thoroughly rinsed with water and then sonicated in ethanol and ultrapure water in turn. The CdS NC film was achieved by dropping 10 μL of CdS NC solution onto the pretreated surface of GCE and evaporated in air at room temperature. The CdS NC modified GCE was stored in $Tris^+$ buffer for characterization and further modification.

**Fabrication of the ECL Aptasensor.** The CdS NC modified GCE was dipped in 2% APS aqueous solution for 45 min. Then, the GCE was rinsed with $Tris^+$ buffer and immersed into 1 mM PDITC *N*,*N*-dimethylformamide (DMF) solution for 2 h. The modified GCE was taken out and incubated in $Tris^+$ buffer containing 0.85 μM aptamer 1 for about 16 h to produce an aptamer/PDITC/APS/CdS attached GCE. Finally, 2 wt % BSA solution was used to block the nonspecific binding sites of the CdS NCs at 4 °C for 1 h. The electrode surface was rinsed with $Tris^+$ buffer after each step to remove nonspecifically adsorbed species.

Then, ssDNA−AuNP conjugates were assembled to the surface of modified GCE via immersing the aptamer-CdS immobilized electrode into 60 μL of ssDNA−AuNP conjugates for the formation of ds-DNA structures between aptamer 1 and ssDNA 1. The hybridization reaction was carried out for 1 h at 37 °C with mechanical shaking. Subsequently, the electrode was washed thoroughly with $Tris^+$ buffer to remove unhybridized ssDNA−AuNP conjugates.

**Analytical Procedure.** Sample solutions containing various concentrations of thrombin were prepared in $Tris^+$ buffer. In a typical test, the assembled aptasensor was incubated in 100 μL of sample solution for 40 min at 37 °C, followed by thoroughly washing with the same buffer to remove unbound thrombin and replaced ssDNA−AuNP conjugates. Before and after the incubation, the ECL responses of the electrode were both recorded in 0.1 M PBS (pH 8.0) containing 0.05 M $K_2S_2O_8$ as a coreactant. The linear scan potential was applied with a scan rate of 100 mV/s, and the voltage of the PMT was set at −500 V. ECL signals related to the thrombin concentrations could be measured.

## RESULT AND DISCUSSION

**Mechanism of ECL Enhancement of the Aptasensor.** The principle of the amplification of ECL aptasensor protocol was shown in Scheme 1. GCE was modified by drop-coating of 10 μL

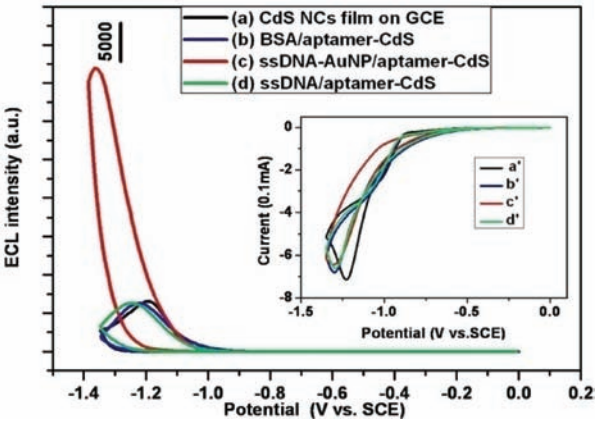


**Figure 1.** Cyclic ECL on potential curves in various cases. (a) CdS NC film on GCE; (b) BSA/aptamer-CdS; (c) ssDNA−AuNP/aptamer-CdS; (d) ssDNA/aptamer-CdS. Inset: the corresponding cyclic voltammograms (CVs): a′ to a; b′ to b; c′ to c; d′ to d. ECL detection buffer: 0.1 M PBS (pH 8.0) containing 0.05 M $S_2O_8^{2-}$. Scan rate, 100 mV $s^{-1}$.

of CdS NCs and used as ECL emitters. The CdS NC film generated an ECL peak in the presence of coreactant $S_2O_8^{2-}$ ions at ca. −1.18 V (Figure 1, curve a). Upon the potential scan with an initial negative direction, the CdS NCs immobilized on the electrode were reduced to nanocrystal species ($CdS^{-\bullet}$) by charge injection, while the coreactant $S_2O_8^{2-}$ was reduced to the strong oxidant $SO_4^{-\bullet}$, and then, $CdS^{-\bullet}$ could react with $SO_4^{-\bullet}$ to emit light in the aqueous solution. The corresponding ECL processes are as follows:[31,32]

$$\text{CdS NCs} + ne \rightarrow n\text{CdS}^{-\bullet} \quad (1)$$

$$S_2O_8^{2-} + e^- \rightarrow SO_4^{2-} + SO_4^{-\bullet} \quad (2)$$

$$\text{CdS}^{-\bullet} + SO_4^{-\bullet} \rightarrow \text{CdS}^* + SO_4^{2-} \quad (3)$$

$$\text{CdS}^* \rightarrow \text{CdS} + h\nu \quad (4)$$

The antithrombin aptamer 1 was immobilized on CdS NC film through the cross-linking of APS and PDITC. The double bond structure of PDITC can effectively expand the distance for the further assembling. As shown in Figure 1, curve b, after the assembling of aptamer 1 on CdS NC film and the subsequent BSA blocking, the ECL emission had a very small change. As a cross-linker, APS could form a layer of silicon atom over the CdS NC film to make the film smoother and hence decrease the nonspecific active binding sites, which could account for the little change of the ECL intensity after BSA blocking. Next, after the hybridization of ssDNA−AuNP conjugates, excitingly, the ECL signal was 5-fold higher than that before hybridization (Figure 1, curve c). However, as shown in Figure 1 inset, the corresponding cyclic voltammograms (CV) showed that the reduction potential of coreactant $S_2O_8^{2-}$ on CdS NC film just had slight negative shift (Figure 1, curve c′), which could be attributed to the negative charges on the surface of Au NPs and oligonucleotides. Besides, the peak current only showed a little decrease after hybridization, which could be explained by the slight inhibition of assembled ssDNA−AuNP conjugates to the coreactant diffusion. Because the amperometic response had little decrease rather than increase, this ECL enhancement could be caused neither by the increased charge transfer rate nor by the interaction of the assembled ssDNA−AuNP conjugates with the coreactant.

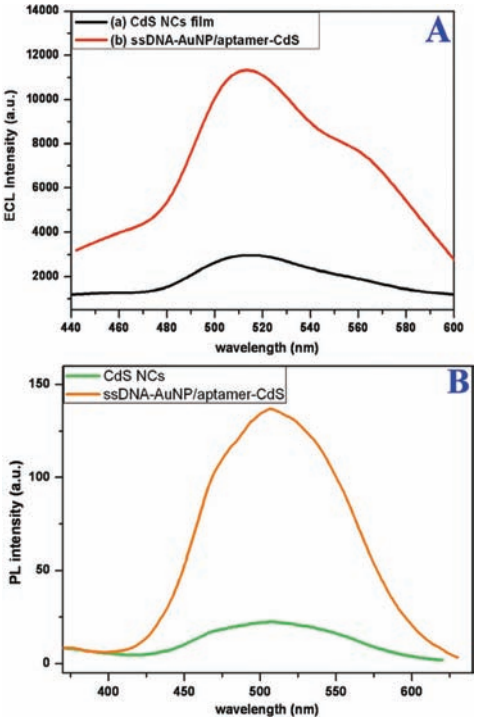


**Figure 2.** (A) ECL spectra of (a) CdS NC film and (b) ssDNA−AuNP/aptamer-CdS in 0.1 M PBS (pH 8.0) containing 0.05 M $S_2O_8^{2-}$ obtained by filter plates. (B) PL spectra of (a) CdS NCs and (b) ssDNA−AuNP/aptamer-CdS in 0.1 M PBS (pH 8.0), excitation wavelength: 380 nm.

To better clarify the ECL enhancement mechanism, a control experiment without the involvement of Au NPs was carried out (Figure 1, curve d). The result displayed that the hybridization between antithrombin aptamer 1 and its complementary ssDNA 1 did not bring any visible enhancement in ECL intensity and did not change the corresponding CV behavior either (Figure 1, curve d′), indicating that this rise of ECL indeed originated from the interaction of CdS NCs and Au NPs. Thus, it may be expected that this dramatic rise of ECL response was due to the energy transfer between CdS NCs and AuNPs.

In order to prove this energy transfer process, we investigated the ECL and PL spectra of CdS NCs before and after assembled ssDNA−AuNP conjugates. A broad ECL emission peaked at ca. 510 nm of CdS NC film was in its ECL spectrum (Figure 2A, curve a). After assembling ssDNA−AuNP conjugates on the CdS NC film, the ECL intensity increased in the full region of ECL spectrum. In addition, in ca. 550−580 nm, the region of lower energy, a shoulder peak obviously increased compared with the original peak of CdS NCs (Figure 2A, curve b). The result indicated the presence of Au NPs could indeed enlarge the ECL of CdS NCs, because Au NPs have hardly any emission under the excitation of 510 nm. PL spectrum was further employed for clarification of the ECL enhancement mechanism (Figure 2B). Compared with that of CdS NCs, it showed 6.3-fold enhancement of PL intensity after assembling ssDNA−AuNP conjugates. The PL enhancement of NCs within the local electromagnetic field produced by the Au NPs has been well documented with the observation of the SPR in the PL excitation


dx.doi.org/10.1021/ac200616g |*Anal. Chem.* 2011, 83, 4004–4011

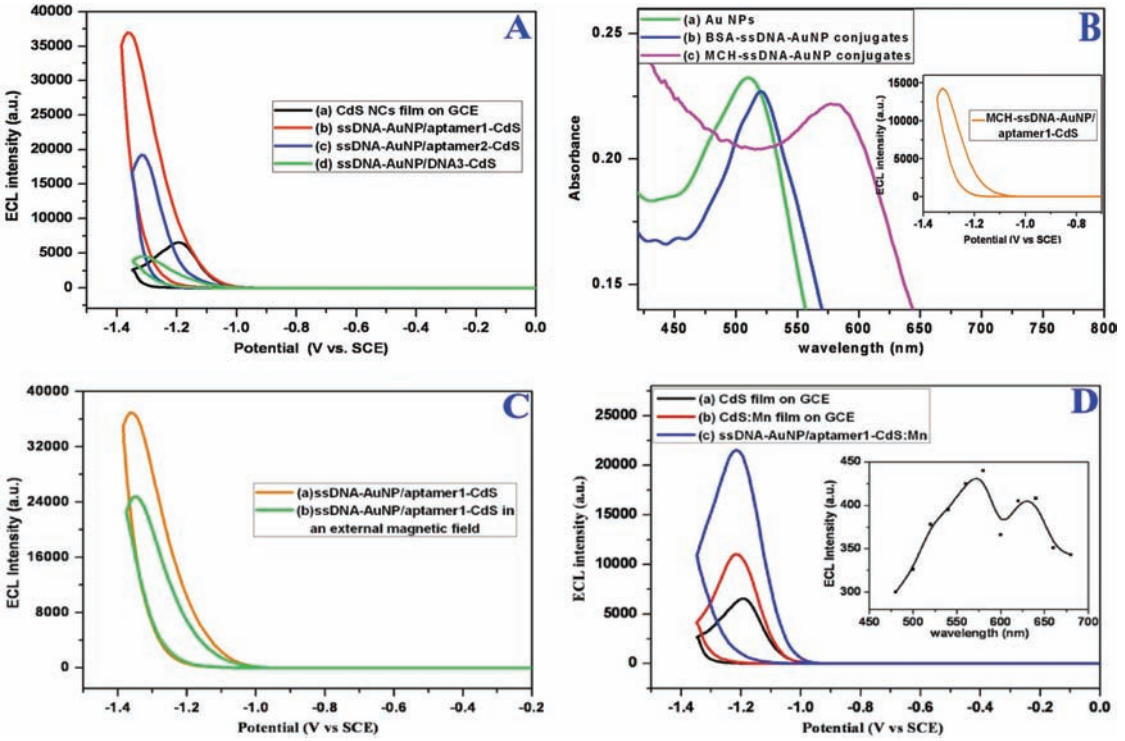


**Figure 3.** (A) Cyclic ECL on potential curves in various cases. (a) CdS NC film on GCE; (b) BSA-ssDNA−AuNP/aptamer1-CdS; (c) BSA-ssDNA−AuNP/aptamer2-CdS; (d) BSA-ssDNA−AuNP/DNA3-CdS; (B) UV−vis absorption spectra of (a) Au NPs; (b) ssDNA−AuNP conjugates blocked with BSA; (c) ssDNA−AuNP conjugates blocked with MCH. Inset: Cyclic ECL of MCH-ssDNA−AuNP/aptamer1-CdS on potential curves. (C) Cyclic ECL of ssDNA−AuNP/aptamer-CdS in the absence (a) and in the presence (b) of an external magnetic field. Magnetic-field strength: 1000 T. (D) Cyclic ECL on potential curves in various cases. (a) CdS NC film on GCE; (b) CdS/Mn film on GCE; (c) MCH-ssDNA−AuNP/aptamer1-CdS/Mn. Inset: ECL spectrum of CdS/Mn NC film. ECL detection buffer: 0.1 M PBS (pH 8.0) containing 0.05 M $S_2O_8^{2-}$. Scan rate, 100 mV $s^{-1}$.

spectrum of NCs.[7,33−36] The slightly larger enhancement of PL (6.3-fold) than that of ECL (5-fold) may due to the additional light absorption in PL except field enhancement. Hence, in our ECL system, the enhancement effect would be dependent on the SPR field of the Au NP enhancement mechanism, namely, the energy transfer of ECL excited SPR in Au NPs to the CdS NCs.

**Influencing Factors on ECL Enhancement.** *Effect of Separation Distance.* The SPR of Au NPs nearby the CdS NC film can be inspired by the ECL emitting; namely, an electromagnetic field was stimulated at the surface of Au NPs. Since the induced SPR spread along the metal surface, with exponential decaying in the vertical direction of the surface,[2,37] SPR related to the distance between the metal and the ECL luminophores. Herein, the ds-DNA structures between the aptamer 1 and ssDNA 1 on Au NPs were applied to control the separation length between CdS NCs and Au NPs effectively. In this case, Au NPs and the CdS NCs were separated by 18 complementary bases and 18 noncomplementary bases (1 nm for 3-base), the separation distance was about 12 nm after hybridization (Figure 3A, curve b). Under the same experimental condition, another control experiment utilizing shorter antithrombin aptamer 2 instead of aptamer 1 and its complementary ssDNA 2 instead of ssDNA 1 was performed. The separation distance decreased from 12 to 9 nm (separated by 12 complementary bases and 15 noncomplementary bases), which resulted in ECL enhancement from 5-fold down to 3-fold (Figure 3A, curve c). We further employed shorter ssDNA 3 and its complementary ssDNA 3′ as the separator between CdS NCs and Au NPs; the separation distance was about 6 nm (18 bases) after hybridization. The ECL intensity decreased rather than enhanced (Figure 3A, curve d), which was a result of FRET, that is to say some ECL excitation energy of CdS NCs was consumed in proximal Au NPs.[19] It has been shown experimentally and theoretically that the competition between FRET and SPR-field enhancement is distance dependent.[2,33] The FRET quenching is a short-range effect, and it would be weakened with the distance much faster than the enhanced SPR field possibly responsible for the enhancement in luminescence. With increasing separation distance, the SPR-field enhancement effect is predominated, while the FRET could be negligible. In this work, the results proved that the SPR field enhanced ECL of CdS NCs by Au NPs could only happen in the larger separate distance, and the enhancement degree was distance dependent.

*Effect of Spectra Overlap.* ECL enhancement efficiency by Au NPs was dependent on the spectral overlap between energy donor and acceptor as well as their separation. Note that a broad ECL emission peaked at ca. 510 nm was obtained in the ECL spectrum of CdS NC film, and ssDNA−AuNP conjugates exhibited an absorption maximum ca. 530 nm (Figure 3B, curve b); the slight red shift of the absorption maximum peak of ssDNA−AuNP conjugates compared with pure Au NPs (Figure 3B, curve a) could be attribute to the change of the Au NP surface charges caused by the oligonucleotides. Obviously, the ECL emission of the CdS NC film has a considerable spectral overlap with SPR absorption of Au NPs. Such overlap would result in the efficient energy transfer from CdS NC film to Au NPs and the subsequent great ECL enhancement. Alternatively, when the 3-mercapto-1-hexanol (MCH) was used for blocking of

nonspecific binding sites of Au NPs instead of BSA, a larger red shift could be observed for this absorption maximum peak of ssDNA−AuNP conjugates at ca. 583 nm (Figure 3B, curve c). Thus, the absorption spectrum of ssDNA−AuNP conjugates blocked with MCH overlapped to a lower extent with ECL emission from CdS NC film. A low efficiency of energy transfer between CdS NC film and Au NPs was expected. Figure 3B, inset, has clearly showed that a much lower ECL enhancement was obtained, which further demonstrated our deduction. Meanwhile, this proved that ECL enhancement was a result of SPR of Au NPs; i.e., ECL could be enhanced only if SPR of Au NPs was sufficiently excited.

*Effect of Magnetic Field.* As is well-known, the luminescence of CdS NCs could be enhanced by the increased local electromagnetic field in close proximal Au NPs, i.e., excited SPR field in Au NPs.[38,39] Hence, we believed this electromagnetic field could be easily affected by the introduction of the extra magnetic field both external and internal. To better demonstrate this magnetic effect, first, we placed CdS NC film with ssDNA−AuNP conjugates into an external magnetic field about 1000 T; an obvious decrease of ECL intensity was observed (Figure 3C), demonstrating the existing of the effect of external magnetic field on the SPR of Au NPs. Second, the magnetic $Mn^{2+}$ doped CdS/Mn NCs were also used as ECL emitters. Owing to the doping of $Mn^{2+}$, two ECL emission peaks can be observed: a broad peak from 530 to 580 nm which is assigned to $Mn^{2+}$-related emission and a peak at 640 nm resulting from CdS NCs surface states (Figure 3D, inset). In order to make sure of the same extent of spectral overlap between QDs ECL emission and SPR absorption of Au NPs as well as the same separate distance, MCH was employed to block the nonspecific binding sites of Au NPs, since the SPR absorption of MCH blocked ssDNA−AuNP conjugates was at ca. 583 nm, which was completely overlapped with the ECL emission spectra of CdS/Mn NCs. Unfortunately, although CdS/Mn NCs have stronger ECL than CdS NCs (Figure 3D, curve b), just only 2-fold enhancement in ECL peak height was observed after assembled MCH blocked ssDNA−AuNP conjugates (Figure 3D, curve c). Compared with the 5-fold enhancement using CdS NCs as emitter, this distinct difference, we think, originated from the internal magnetism of doped $Mn^{2+}$. It indicated that the introduction of extra magnetic field had negative influence on the ECL excited SPR in Au NPs.

**Analytical Performance of the Aptasensor in Thrombin Detection.** Shown in Figure 4 was the ECL signal-time curve under continuous potential scanning for 10 cycles (denoted $I_0$). After the storage in pH 7.4, PBS in the refrigerator at 4 °C for 2 months, the ECL aptasensors showed a quite satisfying stability, which retained about 92% of its initial response. The stable and high ECL signals suggested that this aptasensor possessed good potential cycling stability. On the basis of such an ECL enhancement mechanism, this aptasensor with high ECL signal was very suitable for ultrasensitive determination of target protein, meanwhile, owing to the fact that antithrombin aptamer can bind thrombin with high affinity, and constant interaction between them was stronger than that between ssDNA 1 and the aptamer 1. The ssDNA−AuNP conjugates could be displaced by thrombin, and this event of substitution was monitored by ECL measurements again (denoted $I$). As shown in Figure 5A, the more the displacement took place, the larger ECL intensity reduced. Furthermore, the efficiency of displacement was depended on the concentration of thrombin. The difference of ECL intensity ($\Delta I = I_0 - I$) of the two events could be used to quantify thrombin.

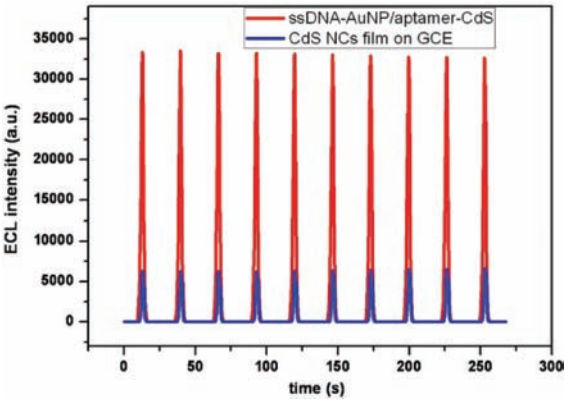


**Figure 4.** Stabilization of ECL emission from (a) ssDNA−AuNP/aptamer-CdS NC film and (b) CdS NC film on GCE in 0.05 M $S_2O_8^{2-}$ + 0.1 M PBS (pH 8.0) under continuous cyclic potential scan for 10 cycles. Scan rate, 100 mV $s^{-1}$.

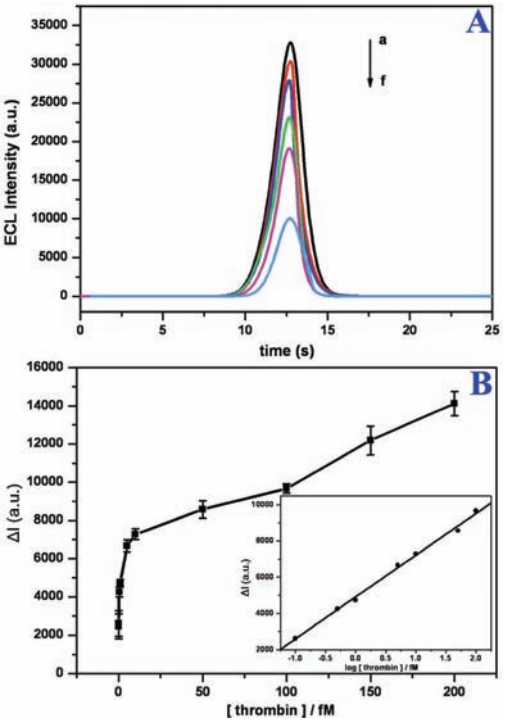


**Figure 5.** (A) ECL signals of the aptasensor incubated with different concentrations of thrombin (from top to down, 0, 0.05, 1, 100, and 200 fM and 1pM, respectively). (B) Relationship between $\Delta I$ and thrombin concentration, three measurements for each point. Inset: logarithmic calibration curve for thrombin.

Figure 5B displayed the relationship between $\Delta I$ and thrombin concentrations (50 aM−200 fM). The $\Delta I$ was found to be logarithmically related to the concentration of thrombin in the range from 100 aM to 100 fM ($R$ = 0.995) with a detection limit of 26 aM at the S/N ratio of 3 (inset in Figure 5B), indicative of an acceptable quantitative behavior, and this ultrasensitive detection at the level of attomolar was much lower than the previously reported ECL detection of thrombin.[22,25−27,40]

The selectivity of the aptasensor for thrombin was tested via comparing the ECL signal changes brought by three other proteins: bovine serum albumin (BSA), hemoglobin (Hb), and lysozyme


dx.doi.org/10.1021/ac200616g |*Anal. Chem.* 2011, 83, 4004–4011

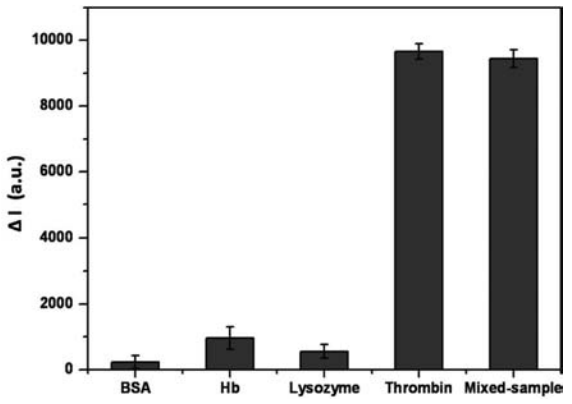


**Figure 6.** Selectivity of the ECL aptasensor to thrombin (0.1 pM) by comparing it to the interfering proteins at the 1 pM level: bovine serum albumin (BSA), hemoglobin (Hb), lysozyme (Lyso), and the mixed sample containing 0.1 pM thrombin and BSA, Hb, and Lyso at the concentrations of 1 pM. The error bars show the standard deviation of three replicate determinations.

(Lyso). Figure 6 compared the ECL responses of the aptasensor after incubation in BSA, Hb, and Lyso solutions under the same experimental conditions and at the same concentration of 1.0 pM. Figure 6 showed that BSA, Hb, and Lyso did not exhibit any great decrease of signal. In contrast to the incubation of the aptasensor into the 0.1 pM thrombin, the intensity greatly decreased (ca. 10 000). Similarly, a mixed sample (0.1 pM thrombin coexisted with 1 pM BSA, Hb, and Lyso) did not exhibit major signal change compared with that of thrombin alone. This comparison essentially suggested that the aptasensor was highly selective and had quite an affinity toward the target protein.

## CONCLUSIONS

This work has demonstrated an ultrasensitive aptasensor based on a 5-fold enhancement of the energy transfer from the ECL-excited SPR in Au NPs to CdS NCs. The successful ECL energy transfer is due not only to their large separation distance but also to their overlapping emission/absorption spectra, and this exciton/SPR of Au NPs can be influenced by external magnetic field or internal magnetic ions easily. With such dramatic amplification signal and the specificity of the aptamers, the concentration detection limits of 26 attomolar for thrombin were obtained. This study opens a new way for S-NCs as energy transfer donor incorporating/inducing SPR of MNPs in ECL bioanalysis. Such ECL aptasensor also offers new opportunities for ultrasensitive detection of biomolecules at very low concentrations, and it is expected to provide new possibilities for protein diagnostics as well as for bioanalysis in general.

## AUTHOR INFORMATION

### Corresponding Author

*E-mail: xujj@nju.edu.cn.

## ACKNOWLEDGMENT

This work was supported by the NSFC (Grant Nos. 21025522, 20975051, 20890021), the NSFC for Creative Research Groups (Grant No. 20821063), and the 973 Program (2007CB936404) of China.

## REFERENCES

(1) Liebermann, T.; Knoll, W. *Colloids Surf., A: Physicochem. Eng. Aspects* **2000**, *171*, 115–130.
(2) Neumann, T.; Johansson, M. L.; Kambhampati, D.; Knoll, W. *Adv. Funct. Mater.* **2002**, *12*, 575–586.
(3) Shimizu, K. T.; Woo, W. K.; Fisher, B. R.; Eisler, H. J.; Bawendi, M. G. *Phys. Rev. Lett.* **2002**, *89*, 117401.
(4) Liu, G. L.; Kim, J.; Lu, Y.; Lee, L. P. *Appl. Phys. Lett.* **2006**, *89*, 241118.
(5) Jin, Y. D.; Gao, X. H. *Nat. Nanotechnol.* **2009**, *4*, 571–576.
(6) Govorov, A. O.; Bryant, G. W.; Zhang, W.; Skeini, T.; Lee, J.; Kotov, N. A.; Slocik, J. M.; Naik, R. R. *Nano Lett.* **2006**, *6*, 984–994.
(7) Matsuda, K.; Ito, Y.; Kanemitsu, Y. *Appl. Phys. Lett.* **2008**, *92*, 211911.
(8) Maye, M. M.; Gang, O.; Cotlet, M. *Chem. Commun.* **2010**, *46*, 6111–6113.
(9) Chen, C. W.; Wang, C. H.; Wei, C. M.; Hsieh, C. Y.; Chen, Y. T.; Chen, Y. F.; Lai, C. W.; Liu, C. L.; Hsieh, C. C.; Chou, P. T. J. *Phys. Chem. C* **2010**, *114*, 799–802.
(10) Anger, P.; Bharadwaj, P.; Novotny, L. *Phys. Rev. Lett.* **2006**, *96*, 113002.
(11) Strekal, N.; Maskevich, A.; Maskevich, S.; Jardillier, J. C.; Nabiev, I. *Biopolymers* **2000**, *57*, 325–328.
(12) Jung, J. M.; Yoo, H. W.; Stellacci, F.; Jung, H. T. *Adv. Mater.* **2010**, *22*, 2542–2546.
(13) Richter, M. M. *Chem. Rev.* **2004**, *104*, 3003–3036.
(14) Jiang, H.; Wang, X. M. *Electrochem. Commun.* **2009**, *11*, 1207–1210.
(15) Miao, W. J.; Bard, A. J. *Anal. Chem.* **2004**, *76*, 5379–5386.
(16) Miao, W. J.; Bard, A. J. *Anal. Chem.* **2004**, *76*, 7109–7113.
(17) Dennany, L.; Forster, R. J.; Rusling, J. F. J. *Am. Chem. Soc.* **2003**, *125*, 5213–5218.
(18) Li, Y.; Qi, H.; Peng, Y.; Yang, J.; Zhang, C. *Electrochem. Commun.* **2007**, *9*, 2571–2575.
(19) Shan, Y.; Xu, J.-J.; Chen, H.-Y. *Chem. Commun.* **2009**, 905–907.
(20) Bae, Y.; Myung, N.; Bard, A. J. *Nano Lett.* **2004**, *4*, 1153–1161.
(21) Sun, L. F.; Bao, L.; Hyun, B. R.; Bartnik, A. C.; Zhong, Y. W.; Reed, J. C.; Pang, D. W.; Abruna, H. D.; Malliaras, G. G.; Wise, F. W. *Nano Lett.* **2009**, *9*, 789–793.
(22) Wang, X. Y.; Dong, P.; Yun, W.; Xu, Y.; He, P. G.; Fang, Y. Z. *Biosens. Bioelectron.* **2009**, *24*, 3288–3292.
(23) Yao, W.; Wang, L.; Wang, H.; Zhang, X.; Li, L. *Biosens. Bioelectron.* **2009**, *24*, 3269–3274.
(24) Yin, X.-B.; Xin, Y.-Y.; Zhao, Y. *Anal. Chem.* **2009**, *81*, 9299–9305.
(25) Fang, L. Y.; Lu, Z. Z.; Wei, H.; Wang, E. *Anal. Chim. Acta* **2008**, *628*, 80–86.
(26) Huang, H. P.; Zhu, J. J. *Biosens. Bioelectron.* **2009**, *25*, 927–930.
(27) Li, Y.; Qi, H. L.; Gao, Q. A.; Yang, J.; Zhang, C. X. *Biosens. Bioelectron.* **2010**, *26*, 754–759.
(28) Tasset, D. M.; Kubik, M. F.; Steiner, W. J. *Mol. Biol* . **1997**, *272*, 688–698.
(29) Gole, A.; Murphy, C. J. *Chem. Mater.* **2004**, *16*, 3633–3640.
(30) Hu, K. C.; Lan, D. X.; Li, X. M.; Zhang, S. S. *Anal. Chem.* **2008**, *80*, 9124–9130.
(31) Myung, N.; Ding, Z. F.; Bard, A. J. *Nano Lett.* **2002**, *2*, 1315–1319.
(32) Jie, G. F.; Liu, B.; Pan, H. C.; Zhu, J. J.; Chen, H. Y. *Anal. Chem.* **2007**, *79*, 5574–5581.
(33) Kulakovich, O.; Strekal, N.; Yaroshevich, A.; Maskevich, S.; Gaponenko, S.; Nabiev, I.; Woggon, U.; Artemyev, M. *Nano Lett.* **2002**, *2*, 1449–1452.
(34) Zayats, M.; Kharitonov, A. B.; Pogorelova, S. P.; Lioubashevski, O.; Katz, E.; Willner, I. J. *Am. Chem. Soc.* **2003**, *125*, 16006–16014.
(35) Lu, L.; Xu, X. L.; Shi, C. S.; Ming, H. *Thin Solid Films* **2010**, *518*, 3250–3254.

(36) Su, X. R.; Zhang, W.; Zhou, L.; Peng, X. N.; Wang, Q. Q. *Opt. Express.* **2010**, *18*, 6516–6521.
(37) Jain, P. K.; Huang, X.; El-Sayed, I. H.; El-Sayad, M. A. *Plasmonics* **2007**, *2*, 107–118.
(38) Biju, V.; Itoh, T.; Anas, A.; Sujith, A.; Ishikawa, M. *Anal. Bioanal. Chem.* **2008**, *391*, 2469–2495.
(39) Sokolov, K.; Chumanov, G.; Cotton, T. M. *Anal. Chem.* **1998**, *70*, 3898–3905.
(40) Zheng, J.; Cheng, G. F.; He, P. G.; Fang, Y. Z. *Talanta* **2010**, *80*, 1868–1872.